Conference Paper

The Study of the Properties of Uranium Dioxide Pellets Depending on the Parameters of Pressing and Sintering

D. P. Shornikov[1], A. V. Tenishev[1], S. N. Nikitin[1], B. A. Tarasov[1], S. V. Starikov[1], A. S. Efimenko[1], I. S. Timoshin[2], and M. E. Matvenov[2]

[1]National Research Nuclear University MEPhI (Moscow Engineering Physics Institute), Kashirskoe shosse 31, Moscow, 115409, Russia
[2]PJSC «Mashinostroitelny Zavod», Elektrostal, Russia

Abstract

The paper presents dilatometric research of uranium dioxide pellets, fabricated by compaction at different pressure values. Temperature observed at sintering start is determined and it is pointed out that this temperature doesn't depend on compaction pressure.

Keywords: uranium dioxide, compaction, sintering, dilatometry, shrink curves, geometric density, pycnometric density.

Corresponding Author:
D. P. Shornikov
d.p.shornikov@mail.ru

Received: 21 December 2017
Accepted: 15 April 2018
Published: 6 May 2018

Publishing services provided by Knowledge E

Selection and Peer-review under the responsibility of the MIE-2017 Conference Committee.

1. Introduction

Uranium dioxide is the primary type of nuclear fuel for commercial reactors. Its fabrication technique consists in compaction of uranium dioxide powder to obtain compacted fuel with subsequent sintering, that said, sintering stage is the most significant as during this very stage final characteristics and dimensions of uranium dioxide pellets are developed [1, 2]. Besides, an important task arises – to determine dependencies linking final physical-chemical characteristics of fuel pellets with initial parameters of powders and modes of their compaction and sintering in order to develop an empirical model of uranium dioxide compaction and sintering.

2. Experiment procedure and test data

To fulfill a set task standard uranium dioxide powder manufactured at PJSC MSZ (Elektrostal) by means of ADU method [3] was used.

At first stage powder microstructure was examined at JEOL 6610 LV scanning electronic microscope. Analysis was performed at scanning electronic microscope in

secondary-electrons and backscattered electrons. Figure 1 (*a* and *b*) presents powder microstructure at different magnification values. Given microstructures clearly show that powder represents granules with average dimensions of about 100 μm, upon that particles shape is not spherical. At high magnification one may observe that granules consist of agglomerates with dimensions of about 5-10 μm, which, in turn, consist of crystalline particles with dimensions of about 100-500 nm.

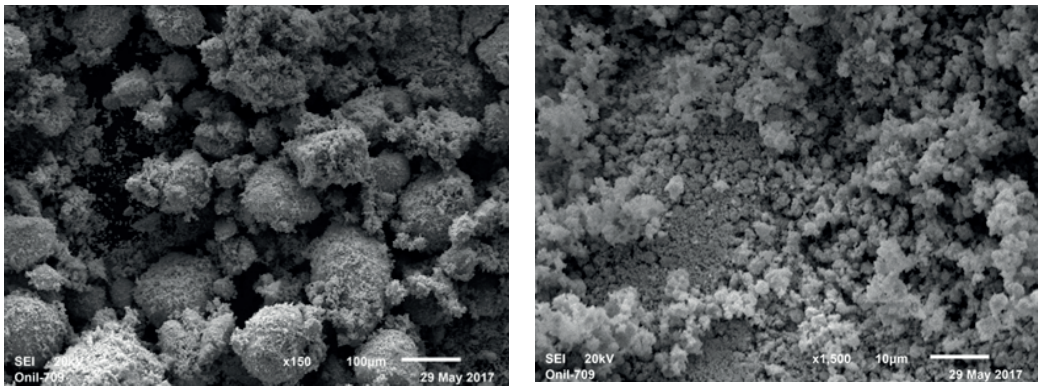

a b

Figure 1: Powder microstructure at different magnification values.

At second stage particles dimensions were examined at Fritsch Analysette 22 laser analyzer. Powder was analyzed in deionized water when exposed to ultrasound with addition of surface-active agent for better particle dispersion. Powder contained agglomerates sizing 0,5-1 mm, which were crushed under ultrasound exposure. Average size of powder particles came to 10-15 μm. Significant part of particles (up to 60%) had size in the range of 1-30 μm. Less than 10% of particles had size below 1 μm. Not more than 30% of powder particles had size in the range of 30-100 μm.

Phase composition before and after sintering was examined at DRON-3M X-ray diffractometer using CuK_{α} radiation. International data base and software (ICDD PDF-2) was used to identify phases. Analysis of obtained diffractograms demonstrated existence of UO_2 peaks and traces of U_3O_8 phase as well. In essence one may point low content of U_3O_8 phase, which may be caused either by slow oxidation of powder when being stored or by initial U_3O_8presence in factory powder. After sintering samples, heated at the rates of 4 and 20 °C/min, were subjected to repeated analysis which demonstrated complete disappearance of U_3O_8 phase.

After that powder was compacted at three pressure values – 2,2; 3,6 and 5,0 t/cm^2. Diameter of pressed pellets came to ~ 6 mm; height - to 4,3-4,5 mm and weight - to ~ 0,7 g. It should be mentioned that plasticizer was not added to pellets in order to reveal kinetics of sintering process. Compacted («green») pellets were measured

for height, diameter and weight, and then geometric density was calculated. Besides, using helium pycnometer, pycnometric volume was determined and pycnometric density was calculated. Functional connection of compact fuel density and compaction pressure is given in Figure 2.

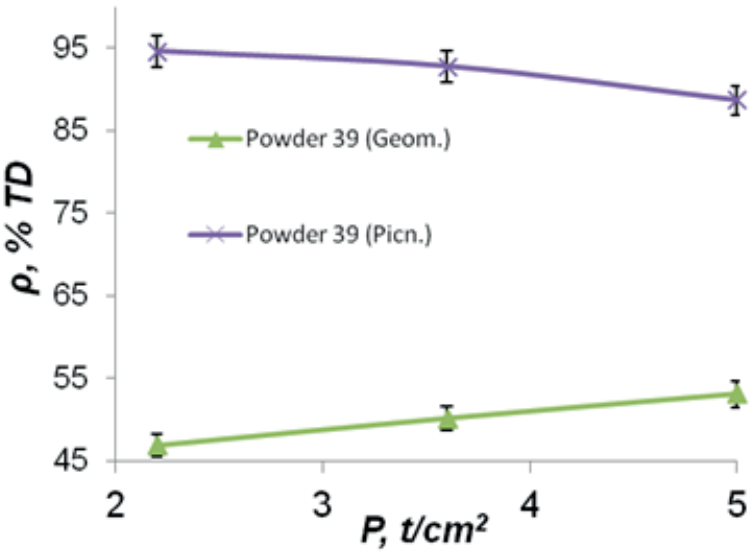

Figure 2: Functional connection of geometric and pycnomentric density and compaction pressure.

As the figure shows, geometric density of «green» compact fuel varies from 45 to 55 % from theoretical density (TD). Increase in compaction pressure up to 5 t/cm^2 doesn't result in destroy of compact fuel after pressing out. It is connected with large number of small particles existing in powder which re-distribute when compacting pellets, fill gaps between UO_2 big particles and eliminate brittle crushing of the latter. Pycnometric density is within the range of 90-95 % from TD, confirming that compact fuel has open porosity mainly. It was observed that pycnometric density decreases with increase of compaction pressure, which has a link to increase of closed porosity portion.

Compacted pellets were heated in Netzsch 402C dilatometer at the rate of 4, 6, 8, 15, 20 °C/min, up to 1600 °C with subsequent dwell at that temperature during 1 h, and then cooling started. Reducing atmosphere with Ar–8 %H_2 flow was used. After sintering linear dimensions and weight, and pycnomentric density of pellets was measured; volume and density were calculated. Consolidated data is given in Figure 3.

Given graphs show that geometric density of pellets increases along with increase of compaction pressure. That said one may observe complicated influence of heating rate on final density, but generally final density increases with decrease of heating rate. Somewhat different situation is observed for pycnometric density. Density decreases at pressure value of 3,6 t/cm^2. Such decrease corresponds to generation of mainly intragranular closed porosity, but pressure value of 2,2 t/cm^2 can be insufficient for

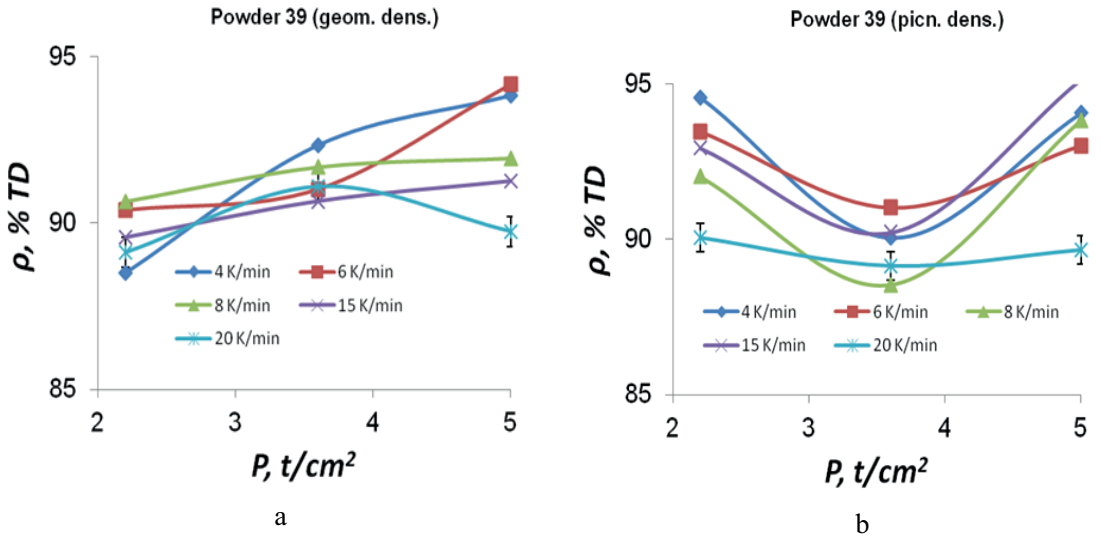

Figure 3: Functional connection of relative density and compaction pressure for powder pertaining to batch 39: *a* – geometric density; 6 – pycnometric density.

generation of mainly closed pores, and pressure value of 5 t/cm^2 could lead to over-pressing of product, that in turn could result in cracks causing through porosity.

Dilatometric curves representing time or temperature dependence of linear shrink of a sample (Δl/l) was analyzed. Linear shrink was re-calculated to volume shrink, then – to density change. After that graphs of density dependence on temperature and time were plotted. Such approach allows future estimation of porosity contribution to sintering process behavior.

Figure 4 demonstrates temperature dependence of density for compact fuel compacted at average pressure of 5,0 t/cm^2.

Given dependences demonstrate that increase of compact fuel density goes along with decrease of heating rate, maximum density (92-94 % TD) can be achieved with rate of 4 °C/min, which is connected with increase in total sintering time. When using high heating rates (20 °C/min) density value comes to ~ 82-85 % and subsequent shrink comes up during isothermic dwell. In all cases sintering starts at ~ 1100 °C. Similar trends are obtained for other compaction pressures as well.

Alongside with density temperature dependence for different compaction pressure values, graphs for shrink of sintered pellets dependence on time were plotted. Availability of such data allows estimation of kinetic parameters of sintering, evaluation of sintering process activation energy and specifying parameters of temperature pattern that can provide sintering with constant rate of shrink. Time dependencies given in Figure 5, include three segments: heating, isothermic dwell and cooling. Shrink curves

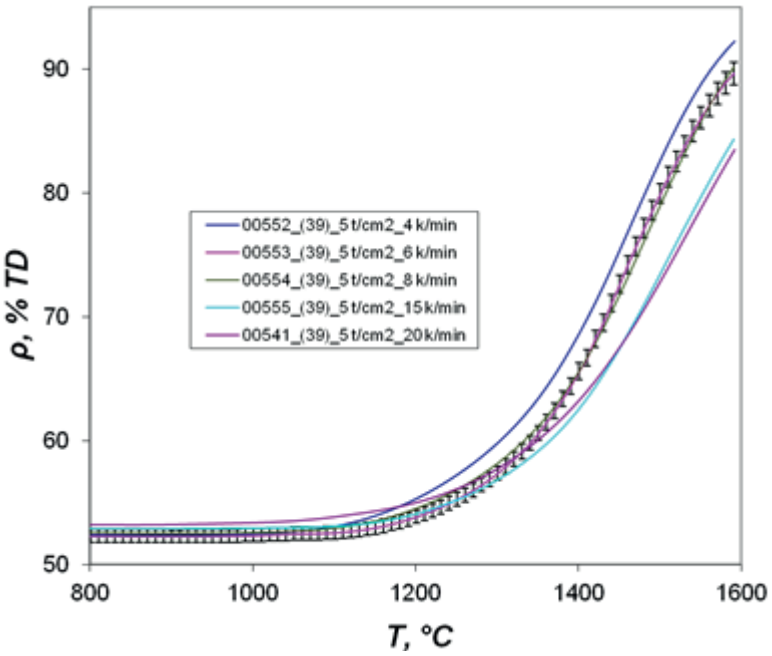

Figure 4: Functional connection of compact fuel relative density and temperature for compaction pressure of 5,0 t/cm^2.

have parts corresponding to isothermic dwell, that allows identifying termination of heating.

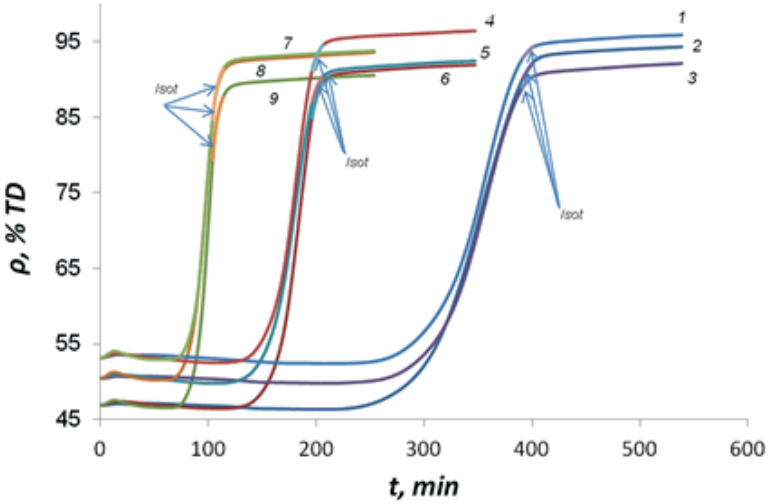

Figure 5: Functional connection of relative density and time: 1 – 5,0 t/cm^2 and 4 °C/min; 2 – 2,2 t/cm^2 and 4 °C/min; 3 – 3,6 t/cm^2 and 4 °C/min; 4 – 5,0 t/cm^2 and 8 °C/min; 5 – 3,6 t/cm^2 and 8 °C/min; 6 – 2,2 t/cm^2 and 8 °C/min; 7 – 5,0 t/cm^2 and 15 °C/min; 8 – 3,6 t/cm^2 and 15 °C/min; 9 – 2,2 t/cm^2 and 15 °C/min; *"isot"* – isothermal segment.

Presented curves demonstrate that the slower heating is, the shallower shrink curve becomes. One can observe evident change of final density depending on applied pressure, for example, 5,0 t/cm^2 causes increase of final density for ~5-7 %, that said, initial

curve run remains constant. Figure 6 illustrates rate of density change depending on time and temperature for three different pressure values with heating rate of 8 °C/min.

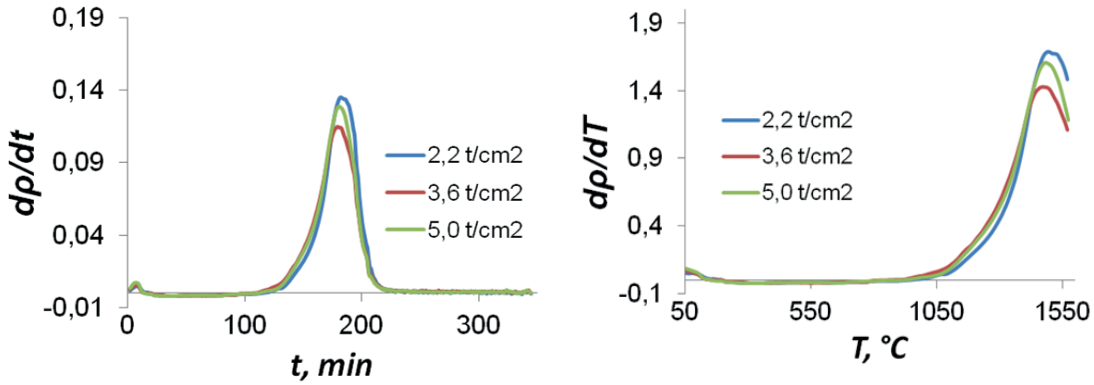

Figure 6: Rate of density change for UO_2 powder pertaining to 39 batch, compacted at pressure values: 2,2; 3,6 and 5,0 t/cm^2 and heating rate: 8 °C/min: a – depending on time; 6 – depending on temperature.

It is clear that compaction pressure has no influence on shrink start, but has influence on shrink rate. Functional connection is rather complicated as the curve has a knee at 1300 °C after which shrink accelerates, and besides minimal shrink rate corresponds to average value of compaction pressure (3,6 t/cm^2).

Presented functional connections clearly demonstrate that sintering kinetics for uranium dioxide depends both on heating rate and applied pressure that said maximum process rate is observed within the range of 1400-1500 ° C.

For more detailed investigation of the process sintering was performed at lower temperatures, with 1 h dwell at 1100, 1300 and 1450 °C. Compaction pressure came to 3,6 t/cm^2, and heating rate - to 15 °C/min. Obtained time dependences of samples densities are given in Figure 7.

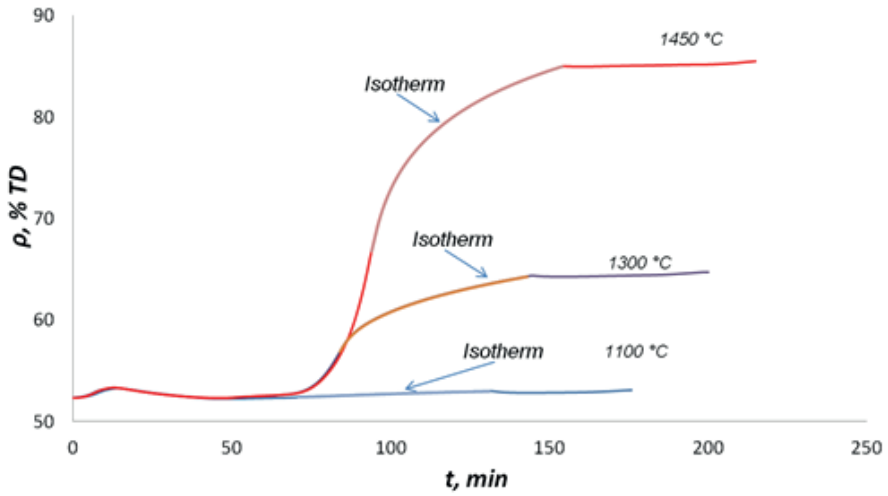

Figure 7: Functional connection of relative density and time for compaction pressure of 3,6 t/cm^2 and temperature of 1100, 1300 and 1450 °C.

Presented functional connections demonstrate that sintering starts at ~ 1100 °C and final density of product increases with increase of dwell temperature. Though data given in Figure 7 shows that at 1100 °C almost no shrink happens whereas at higher temperatures density increases as time passes, but process rate quickly reduces. Consequently keeping of process rate requires constant overheating.

3. Results and discussion

Analysis of obtained dilatometric curves allows making an important practical conclusion: increase of compaction pressure leads to increase of final density of sintered product. That said shrink kinetics depends both on compaction pressure and heating rate of compact fuel when sintering. High heating rate (15 °C/min) leads to some reduction (2-4 %) in final density, but hereby analysis of isothermic parts of curves 7-9 in Figure 5 demonstrates that in this case high shrink rate could be kept at isothermal dwell, which allows achieving density of ~ 95 % owing to elongation of the latter.

It can be concluded that compaction and consequently microstructure of a final pellet will be determined by powder particles' size, which is connected with mechanisms of plastic strain, plastic flow [4] and diffusive mass transfer, compaction pressure, heating rate, and maximum sintering temperature as well as dwell period at this temperature. Increase of heating rate leads to decrease of diffusive mass transfer contribution at same temperatures and increase of temperature of shrink start [5–7]. Analysis of derivatives presented in Figure 6 demonstrates complicated dependence of shrink rate on compaction pressure. Currently it represents a curve with minimum. Therefore each powder requires specification of best values for above mentioned parameters which asks for generation of empirical model of sintering process and at a later stage – its physical model.

Later obtained data will be supplemented with behavior analysis of powder, fabricated at dry conversion plant, and with microstructure research which will allow doing next step to understanding of investigated processes.

4. Conclusion

1. Functional connection of compact fuel density and compaction pressure of 2,2, 3,6 and 5 t/cm^2 was obtained. It was demonstrated that geometric density increases with increase of pressure and falls in the range of 45-55 % TD, whereas pycnometric density reduces and falls in the range of 95-90 % from TD, which confirms that compact fuel has mainly open porosity.

2. Results of sintering performed in dilatometer with different heating rates demonstrated that final (geometric) density of pellets increases with increase of compaction pressure but at the same time it was observed that pycnometric density decreased at pressure value of 3,6 t/cm^2, that could be explained by formation of closed porosity mainly.

3. Functional connections of temperature and time with density for fuels compacted at different pressures were obtained. Sintering starts at ~ 1100 °C. Density increases with decrease of heating rate, which is connected with elongation of total sintering time. Besides as heating rate decreases, shrink curve becomes shallower. Compaction pressure has no influence on shrink start but has influence on its rate that said dependence is complicated, with obvious minimum.

4. Sintering of UO_2 powder at lower temperatures: 1100, 1300 and 1450 °C demonstrated that final product density increases with increase of temperature. When dwelling at 1100 °C almost no shrink occurs but at higher temperatures density increases as time passes and process rate quickly decreases. Consequently process rate keeping requires constant overheating.

ACKNOWLEDGMENTS

"Presented research was performed with the assistance of State assignment of RF Ministry of Education and Science (Project 11.2594.2017/4.6)".

This work was supported by the MEPhI Academic Excellence Project (agreement with the Ministry of Education and Science of the Russian Federation of August 27, 2013, project no. 02.a03.21.0005).

References

[1] Advanced fuel pellet materials and designs for water cooled reactors *IAEA-TECDOC-1416, IAEA*, Vienna, 2004.

[2] Kotelnikov R.B., Bashlykov S.N., Kashtanov A.I.. Menshikova T.S. High-temperature nuclear fuel Atomizdat, 1978, 432 p.

[3] Majorov A.A., Braverman I.B. The technology of obtaining powders of ceramic uranium dioxide *Energoatomizdat* 1985, 127 p.

[4] Baranov, V.G., Devyatko, Yu.N., Tenishev, A.V., Khlunov, A.V., Khomyakov, O.V. Sintering of oxide nuclear fuel: Plastic flow mechanism. (2013) *Journal of Nuclear Materials* 432 (1-3) PP. 52 - 56 http://dx.doi.org/10.1016/j.jnucmat.2012.07.050

[5] Wilkinson D.S., Ashby M.F. Pressure sintering by power law creep *Acta Metallurgica*. 1975. Vol. 23. Is. 11. P. 1277-1285

[6] Baranov, V.G., Kuzmin, R.S., Tenishev, A.V., Khlunov, A.V., Ivanov, A.V., Petrov, I.V., Timoshin, I.S. Sintering parameters for uranium-gadolinium oxide fuel pellets. (2012) *Atomic Energy* 112 (4) PP. 303 - 306 http://dx.doi.org/10.1007/s10512-012-9561-2

[7] Baranov, V.G., Kuzmin, R.S., Tenishev, A.V., Khlunov, A.V., Ivanov, A.V., Petrov, I.V., Timoshin, I.S. Sintering particulars of pelletized oxide nuclear fuel. (2011) *Atomic Energy* 110 (3) PP. 172 - 177 http://dx.doi.org/10.1007/s10512-011-9407-3